SOIL DEGRADATION ASSESSMENT USING GEOINFORMATICS TECHNOLOGY IN UPPER LAMCHIENGKRAI WATERSHED, NAKHON RATCHASIMA PROVINCE, THAILAND

Sasikarn Plaiklang and Suwit Ongsomwang*

Received: November 13, 2017; Revised: December 04, 2017; Accepted: December 13, 2017

Abstract

Soil erosion and soil salinity are major environmental problems in Thailand because they create seriously negative impacts on agricultural and environmental sustainability. In addition, soil erosion leads to the depletion of organic matter in soil. In the meantime, soil erosion, salinity, and organic matter depletion are significant indicators for a soil degradation assessment. The main objectives of the study were (1) to classify land use and land cover, (2) to assess soil loss and its severity, (3) to assess soil salinity and its severity, (4) to assess soil organic matter and its depletion, and (5) to assess soil degradation and its severity. In this study, the LULC classification using the decision tree classifier, soil erosion with the RMMF model, soil salinity and depletion of organic matter content with linear and non-linear regression analysis were firstly analyzed separately and their results then were combined to evaluate soil degradation using the multiplication method. For the results, an optimum CART model, which applied blue, green, red, NIR, SWIR-1, SWIR-2 bands, wetness index, and elevation to construct a decision tree for LULC classification from Landsat 8 images and DEM, provided an overall accuracy at 87.50% and a Kappa hat coefficient at 80.10%. Meanwhile, the average erosion rate in the study area was 3.37 ton/ha/year. The most dominant soil erosion severity class was very slightly eroded (<6.25 ton/ha/year) and it covered an area of 437.70 km^2 or about 94.14% of the total study area. In the meantime, the most dominant soil salinity severity class was very low and covered an area of 415.55 km^2 or about 89.37% of the total study area. At the same time, the dominant soil biological degradation class was moderate and covered an area of 296.05 km^2 or 63.67% of the total study area. According to the soil degradation assessment using the multiplicative method, the most dominant soil degradation class was very low and covered

---

School of Remote Sensing, Institute of Science, Suranaree University of Technology, Nakhon Ratchasima 30000, Thailand. E-mail: suwit@sut.ac.th

* *Corresponding author*

area of 443.00 km^2 or 95.28% of the total study area. These findings implied that a serious problem of soil degradation did not exist in the study area. In conclusion, it appeared that geoinformatics technology can be efficiently used as a tool to assess soil loss, soil salinity, and soil organic matter depletion and their severities for a soil degradation assessment.

Keywords: Soil degradation assessment, RMMF model, soil salinity index, soil color index, Upper Lamchiengkrai watershed, Nakhon Ratchasima, Thailand

Introduction

Land degradation is a worldwide serious environmental problem (United Nations Environment Programme, 2006). It has harmful impacts on agricultural productivity and ecological functions that ultimately affect human sustenance and quality of life (Mhangara, 2011). The most critical component of land degradation is soil degradation (Mainguet, 1994, quoted in Denti, 2004). Soil degradation is a decline in soil quality encompassing deterioration in the physical, chemical, and biological attributes of the soil (Eaton, 1996). Indicators of soil degradation are soil erosion, soil salinity, decline of soil structure, and nutrient depletion (Lal, 1998). In Thailand, soil erosion and soil salinity are major problems because they create seriously negative impacts on agricultural land and environmental sustainability (Land Development Department, 2002; Katawatin and Sukchan, 2012) and they are also harmful to people and the environment (Jumpa, 2012). In addition, soil erosion leads to the depletion of organic matter in soil (Food and Agriculture Organization of the United Nations, 2005).

According to the global report of land degradation by Bai *et al.* (2008) it was found that the area of degraded land in Thailand was 0.895% of the global degraded area. In addition, a statistical report on soil degradation assessment by the Land Development Department (LDD) in 2015 revealed that 56.8% of the total area or about 291200 km^2 in Thailand was degraded. The report showed an increasing trend of soil degradation and the major causes included an increasing population, deforestation, unsuitable land use, and a lack of improvement of soil quality. Sethabut (2008) suggested that the Thai government should recognize the soil degradation problem for mitigation and prevention of the problem in both the short term and long term. Soil degradation assessment is mostly based on in situ soil surveys (Kapalanga, 2008) which can provide the most accurate data (Torrion, 2002), However, the procedure is costly and time consuming (Harmsen, 1996, quoted in Yazidhi, 2003) and it is also difficult to detect wide and inaccessible areas (Bai *et al.*, 2008).

Huete (2004) mentioned that general information and data regarding the spatial extent and severity of soil degradation are poorly understood and the available data are limited. Actually, the traditional approach based on field data collection is expensive, takes a long time, and is hardly reproducible (Abbas and Khan, 2007). To solve the problem of soil degradation for field data collection on a local scale, proper approaches for soil degradation assessment are required (Bai *et al.*, 2008).

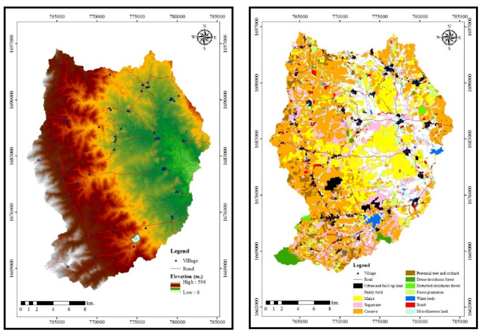

(a) (b)

Figure 1. Study area: (a) topography data and (b) land use data of LDD

Geoinformatics technology is a very important tool for decision-making across a wide range of disciplines. It is a basal and essential technical core of the system for assessing geospatial information and monitoring the environment (Fadhil, 2009). It is also used to assess and monitor soil degradation (Kapalanga, 2009), to measure variables linked to soil degradation (Prince, 2002, quoted in Mambo and Archer, 2006), to provide time series data for monitoring land cover change (Lillesand *et al.*, 2004), and to detect wide and inaccessible areas (Torahi, 2012).

This study aims to develop a new approach using geoinformatics technology to assess the extent and severity of soil degradation. The specific objectives of the study were (1) to classify land use and land cover (LULC), (2) to assess soil loss and its severity, (3) to assess soil salinity and its severity, (4) to assess soil organic matter and its depletion, and (5) to assess soil degradation and its severity.

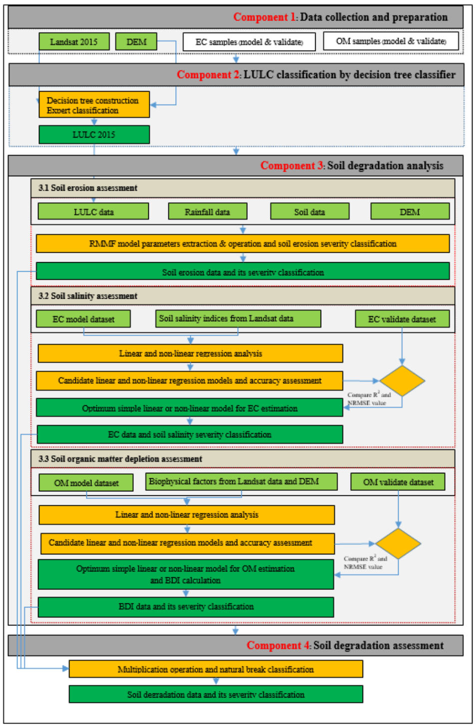

Figure 2. Workflow diagram of the research methodology

Materials and Method

Study Area

The study area is the Upper Lamchiengkrai watershed which originates from a mountainous area in Bamnet Narong district, Chaiyaphum province. It covers 3 districts of Nakhon Ratchasima province comprising Theparak, Dan Khun Thot, and Si Khiu and it covers an area of 464.96 km^2. The elevation of the study area ranges approximately from 0 m to 596 m (Figure 1(a)). According to land use data in 2015 of the LDD, the eastern part of the study area, where major economic crops including paddy fields, cassava, maize, and sugarcane are situated, is mostly flat. On the contrary, the western part of the study area is undulating with mountainous areas and is mostly covered with cassava (Figure 1(b)). The tributaries of the existing rivers in the study area flow from west to east.

Research Methodology

The research methodology consisted of 4 components: (1) data collection and preparation, (2) LULC classification by a decision tree classifier, (3) soil degradation analysis, and (4) soil degradation assessment (Figure 2).

Data Collection and Preparation

Basic remotely sensed data and bio-physical data were collected and prepared for analysis and modeling (Table 1).

LULC Classification by Decision Tree Classifier

Supervised classification with the decision tree classifier by the classification and regression tree (CART) algorithm and expert system was here applied to classify the LULC types in 2015. In practice, the selected influential factors on the LULC type and the distribution as independent variables, which included spectral data of Landsat 8 images and derived indices (brightness, greenness, and wetness) and physical factors (elevation, slope, and aspect), were firstly prepared from training areas to extract a decision tree structure for the LULC classification using SPSS statistics software, and the derived decision tree was further migrated to the Knowledge Engineer module of ERDAS Imagine software for the LULC classification. The LULC classification system, which was modified from the land use classification scheme of the LDD, consisted of (1) urban and built-up area (URBAN), (2) paddy field (PF), (3) maize (MAIZE), (4) sugarcane (SGC), (5) cassava (CAS), (6) perennial tree and orchard (TREE), (7) dense deciduous forest (DDF), (8) disturbed deciduous forest (DIDF), (9) forest plantation (PF), (10) water body (WATER), (11) scrub (SCRUB), and (12) miscellaneous land (MISC). In addition, accuracy assessment of the thematic LULC map was performed based on reference LULC data from a field survey in 2015 using overall accuracy, producer's accuracy, user's accuracy, and Kappa hat coefficient of agreement.

Soil Degradation Analysis

Soil degradation analysis, which included soil erosion, soil salinity and soil organic matter depletion assessment, was processed under the ESRI ArcGIS environment. In practice, the Model Builder module of ESRI ArcGIS was applied for semi-automatic processing of the soil degradation assessment.

Soil Erosion Assessment

Soil erosion, which represents a physical indicator for soil degradation, was assessed using the revised Morgan-Morgan-Finney (RMMF) model that was developed by Morgan in 2001. In practice, the LULC data for the proportion of rainfall intercepted by crop cover, percentage canopy cover, plant height, ratio of actual to potential evapotranspiration, percentage ground cover, crop cover management, effective hydrological depth of soil, rainfall data for annual rainfall total, intensity of erosive rain, number of rain days per year, soil data for soil moisture content at field capacity, bulk density of top soil, soil detachment index, and cohesion of the surface soil and digital elevation model (DEM) data for slope steepness were prepared to extract the RMMF parameters. In this study, some RMMF model parameters were directly extracted based on the prepared data including

Table 1. List of data collection and preparation

Data collection	Data Preparation	Source	Year
Landsat data: Path 129 Row 49	Completeness checking	USGS	9 March 2015
Administrative boundary	Completeness checking	DEQP	2011
DEM	Completeness checking	USGS	2014
Slope	Extract from DEM		
Aspect	Extract from DEM		
Rainfall	Surface interpolation	TMD	1985-2015
Soil series	Completeness checking	LDD	1999
Brightness	Create from Landsat data		
Greenness	Create from Landsat data		
Wetness	Create from Landsat data		
NDVI	Create from Landsat data		
NDWI	Create from Landsat data		
Spectral soil salinity indices	Create from Landsat data		
Spectral soil color indices	Create from Landsat data		
Soil salinity sampling points	Soil sample analysis	Field survey/Laboratory	2015-2016
Soil organic matter sampling points	Soil sample analysis	Field survey/Laboratory	2015-2016

USGS: United States Geological Survey; DEQP: Department of Environmental Quality; TMD: Thai Meteorological Department; LDD: Land Development Department annual rainfall total, number of rain days per year, and slope steepness, while others were assigned based on literature reviews from Morgan (2001); Yazidhi (2003); Morgan and Duzant (2008); Suriyaprasit (2008); and Kamonrat and Jirakajohmkool (2012). For the soil erosion estimation, 5 operating functions of the RMMF model comprising (a) estimation of rainfall energy, (b) estimation of annual runoff, (c) estimation of soil particle detachment, (d) estimation of transport capacity of runoff, and (e) estimation of soil loss were implemented (Figure 3). In addition, the list of the applied equations of the RMMF model is summarized in Table 2. Finally, the result of the soil erosion assessment using the RMMF model was further classified for its severity according to the standard of the LDD (2000).

Soil Salinity Assessment

Soil salinity, which presents a chemical indicator for soil degradation, was assessed using an optimum linear or non-linear model for the soil electric conductivity (EC) estimation. In practice, soil samples consisting of modeling (60%) and validating (40%) datasets over the

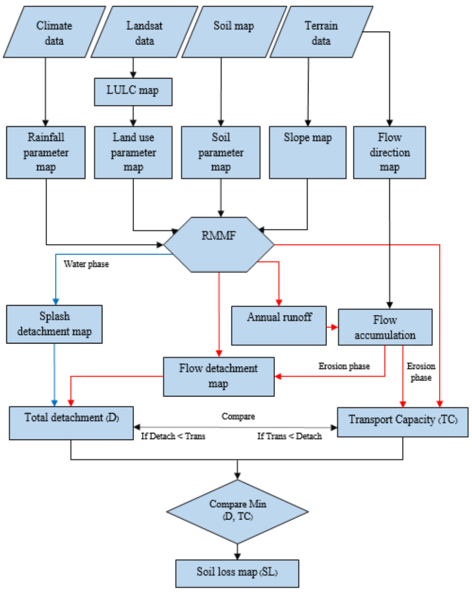

Figure 3. Workflow diagram of RMMF model (Modified from Yazidhi, 2003)

combination of the LULC and soil series data were firstly collected using a soil auger at the topsoil level (0-30 cm) and they were further analyzed to extract the EC data using the EC 1:5 method at the laboratory of Suranaree University of Technology (SUT). After that, an EC estimation model was developed using linear and non-linear regression analysis based on the modeling dataset. The spectral salinity indices (NDSI, SI1, SI2, SI3, S1, S2, S3, S4, S5, and S6) as independent variables were firstly extracted from the Landsat 8 data in 2015 according to its equation (Table 3) while the analyzed EC data that imply the soil salinity level were used as the dependent variable. General equation forms for the EC estimation model development under linear or non-linear regression analysis included:

(1) Simple linear model: $Y = b_0+(b_1*X)$ (1)

(2) Multiple linear model: $Y = b_0+(b_1*X_1)+(b_2*X_2)+(b_3*X_3)+\ldots(b_n*X_n)$ (2)

(3) Logarithmic model: $Y = b_0+(b_1*\ln(X))$ (3)

(4) Inverse model: $Y = b_0+(b_1/X)$ (4)

(5) Quadratic model: $Y = b_0+(b_1*X)+(b_2*X**2)$ (5)

(6) Cubic model: $Y = b_0+(b_1*X)+(b_2*X**2)+(b_3*X**3)$ (6)

(7) Power model: $Y = b_0*(X**b_1)$ (7)

(8) Compound model: $Y = b_0*(b_1**X)$ (8)

(9) S-curve model: $Y = e**(b_0+(b_1/X))$ (9)

(10) Growth model: $Y = e**(b_0+(b_1*X))$ (10)

(11) Exponential model: $Y = b_0*(e**(b_1*X))$ (11)

where, X is the independent variables and Y is the dependent variable.

The derived equations of the linear and non-linear equations, which provide the coefficient of determination (R^2) equal to or more than 0.5, were used as candidate equations to identify an optimum model for the EC estimation from the analyzed EC validation dataset based on the lowest normalized root mean square error (NRMSE) with the following equations:

$$RMSE = \sqrt{\frac{1}{n}\sum_{i=1}^{n}[Estimated\ value - Observed\ value]^2} \quad (12)$$

$$NRMSE = \frac{RMSE}{Maximum\ observed\ value - Minimum\ observed\ value} \quad (13)$$

where RMSE is the root mean square error and n is the number of observations. Finally, the optimum EC estimation model from the linear or non-linear regression analysis was applied to create EC data and the derived result was further classified for soil salinity severity based on the combination between the EC value and soil texture as suggested by Patterson (2006) (Table 4).

Soil Organic Matter Depletion Assessment

Like the soil salinity analysis, soil organic matter (OM) depletion, which presents a biological indicator for soil degradation, was

Table 2. Operating function for the RMMF model

Eq.	Function name	Symbol	Equation	Parameter description
1	Effective rainfall	ER	$ER = R*A$	ER = Effective rainfall (mm)
2	Leaf drainage	LD	$LD = ER*CC$	LD = Leaf drainage (mm)
3	Direct through fall	DT	$DT=ER-LD$	DT = Direct through fall (mm)
4	Kinetic energy of direct through fall	KE(DT)	$KE(DT) = DT*(11.9+8.7 \text{ Log}_{10} I)$	KE (DT) = Kinetic energy of direct through fall (J m^{-2})
5	Kinetic energy of leaf drainage	KE(LD)	$KE(LD) = LD*(15.8*PH^{0.5})-5.87$	KE(LD) = Kinetic energy of leaf drainage (J m^{-2})
6	Kinetic energy of rainfall	KE	$KE = KE(DT)+KE(LD)$	KE = Kinetic energy of rainfall (J m^{-2})
7	Soil moisture storage capacity	Rc	$Rc = 1000*MS*BD*EHD*(Et/Eo)^{0.5}$	Rc = Soil moisture storage capacity (mm)
8	Mean rain per day	Ro	$Ro = R/Rn$	Ro = Mean rain per day (mm)
9	Annual runoff	Q	$Q = R*\exp(-Rc/Ro)$	Q = Annual runoff (mm)
10	Soil particle detachment by raindrop impact	F	$F=K*KE*10^{-3}$	F = Soil particle detachment by raindrop impact (kg m^{-2})
11	Soil resistance	Z	$Z = 1/(0.5*COH)$	Z = Soil resistance (unitless)
12	Runoff detachment	H	$H = ZQ^{1.5} \sin S (1-GC)*10^{-3}$	H = Runoff detachment (kg m^{-2})
13	Total particle detachment	D	$D = F+H$	D = Total particle detachment (kg m^{-2})
14	Transport capacity of runoff	TC	$TC = CQ^2 \sin S * 10^{-3}$	TC = Transport capacity of runoff (kg m^{-2})
15	Annual soil loss	SL	$SL = \text{Minimum} (D, TC)$	SL = Annual soil loss (kg m^{-2})
				R = Annual rainfall total (mm) A = Proportion of rainfall intercepted by crop cover (0-1) Rn = Number of rain days in a year (days) I = Rainfall intensity (mm h^{-1}) CC = Percentage canopy cover (%) PH = Plant height (m) MS = Soil moisture content at field capacity (ww%) BD = Bulk density (g cm^{-3}) EHD = Effective hydrological depth of soil (m.) Et/Eo = Ratio of actual to potential evapotranspiration (unitless) K = Soil erodibility (g j^{-1}) S = Slope steepness (degree) GC = Ground cover (%) COH = Cohesion of the surface soil (k Pa) C = Crop cover management (unitless)

Source: Modified from Yazidhi (2003)

here assessed using an optimum linear or non-linear model for the OM estimation. The soil samples of the OM (model and validated datasets) over the combination of the LULC and soil series data were firstly collected using a soil auger at topsoil level (0-30 cm) and they were further analyzed, using the Walkley and Black method at the SUT laboratory, for OM extraction. After that, the OM estimation model was developed using linear and non-linear regression analysis. In this study, the brightness value of bands 2-7 of the Landsat 8 data, soil color indices (brightness index, coloration index, hue index, redness index, and saturation index), normalized different vegetation index (NDVI), normalized different water index (NDWI), and slope and aspect as independent variables were firstly extracted according to the equation (Table 5) while the analyzed OM data from the modeling dataset was used as the dependent variable. The derived equations of the linear and non-linear models (Equations 1 to 11), which provide the R^2 equal to or more than 0.5, were used as the candidate equations to identify an optimum model from the analyzed OM validation dataset based on the lowest NRMSE. Then, the optimum OM estimation model was further applied to create OM data and it was normalized using the linear scale transformation method ranging between 0 and 1 (Singh *et al*., 2015) using the following equation:

$$\hat{X}=\frac{X\text{-}Xmin}{Xmax\text{-}Xmin} \quad (14)$$

Table 3. Lists of spectral salinity indices

Salinity indices	Equation	Note	Reference
NDSI	$NDSI = \frac{R\text{-}NIR}{R\text{+}NIR}$	B is blue reflectance flux G is green reflectance flux R is red reflectance flux NIR is near infrared reflectance flux	Khan *et al*. (2005)
SI1	$SI1 = \sqrt{G \times R}$		Douaoui *et al*. (2006)
SI2	$SI2 = \sqrt{G^2 \times R^2 \times NIR^2}$		Douaoui *et al*. (2006)
SI3	$SI3 = \sqrt{G^2 \times R^2}$		Douaoui *et al*. (2006)
S_1	$S_1 = B/R$		Abbas and Khan (2007)
S_2	$S_2 = (B - R)/(B + R)$		Abbas and Khan (2007)
S_3	$S_3 = (G \times R)/B$		Abbas and Khan (2007)
S_4	$S_4 = \sqrt{B \times R}$		Abbas and Khan (2007)
S_5	$S_5 = (B \times R)/ G$		Abbas and Khan (2007)
S_6	$S_6 = (R \times NIR)/G$		Abbas and Khan (2007)

Table 4. Severity class of soil salinity (Patterson, 2006)

Level of soil salinity	Effect on Plant Growth	EC of 1:5 soil/water extract (dS m^{-1})				
		sand/ loamy sand	loam	sandy clay loam	light clay	heavy clay
Very low	negligible effect	<0.15	<0.17	<0.25	<0.30	<0.40
Low	very sensitive crops affected	0.16-0.30	0.18-0.35	0.26-0.45	0.31-0.60	0.41-0.80
Moderate	many crops affected	0.31-0.60	0.36-0.75	0.46-0.90	0.61-1.15	0.81-1.60
High	salt tolerant plants grow	0.61-1.20	0.76-1.50	0.91-1.75	1.16-2.30	1.61-3.20
Very High	few salt tolerant plants grow	>1.20	>1.50	>1.75	>2.30	>3.20

where, $\hat{X}$ is the normalized value, X is the actual value, $Xmin$ is the minimum of the actual value, and $Xmax$ is the maximum of the actual value. Later, the normalized values of the OM were converted to percent by multiplication by 100. After that, the biological degradation index (BDI), that represents the depletion of the soil organic matter content, was calculated as suggested by De Paz *et al.* (2006) with the following equation:

$$BDI=\frac{1}{OM} \quad (15)$$

where, BDI is the biological degradation index and OM is the organic matter content (%). Finally, the BDI was further equal interval classified for soil biological degradation into 5 classes with modification of the suggestion of De Paz *et al.* (2006) (Table 6).

Soil Degradation Assessment

Multiple indicators (soil erosion, soil salinity, and soil biological degradation) on soil degradation were here combined using the multiplicative method for soil degradation assessment. In this study, the derived soil loss, the estimated soil salinity, and BDI data were firstly separately normalized using the linear scale transformation method (Equation 14). Then, the normalized data of the 3 indicators were multiplied together and reclassified into 5 soil degradation severity classes (very low, low, moderate, high, and very high) using the natural break method.

Results and Discussion

Optimum CART Model for LULC Classification and Its Result

An optimum CART model applied blue, green, red, NIR, SWIR-1, SWIR-2, wetness, and elevation data as the final criteria to construct a decision tree for the LULC classification (Figure 4). The binary decision tree structure consisted of 59 nodes that included 30 terminal nodes with labelled LULC classes by a sequence

Table 5. Lists of spectral color indices

Spectral color indices	Equation	Note	Reference
Brightness index (BI)	$BI=\sqrt{\frac{(B^2+G^2+R^2)}{3}}$	B is blue reflectance flux G is green reflectance flux R is red reflectance flux NIR is near infrared reflectance flux SWIR is shortwave infrared reflectance flux	Mathieu and Pouget (1998)
Coloration index (CI)	$CI=\frac{R-G}{R+G}$		Mathieu and Pouget (1998)
Hue index (CI)	$HI=\frac{2*R-G-B}{G-B}$		Mathieu and Pouget (1998)
Redness index (RI)	$RI=\frac{R^2}{(B-G^3)}$		Mathieu and Pouget (1998)
Saturation index (RI)	$SI=\frac{R-B}{R+B}$		Mathieu and Pouget (1998)
Normalized different vegetation index (NDVI)	$NDVI=\frac{NIR-R}{NIR+R}$		Rouse *et al.* (1974)
Normalized different water index (NDWI)	$NDWI=\frac{NIR-SWIR}{NIR+SWIR}$		Gao (1996)

Table 6. Biological degradation index and its classification with equal interval method

	Level of soil biological degradation				
	Very low	Low	Moderate	High	Very high
BDI	≤0.0125	0.0125-0.0167	0.0167-0.0250	0.0250-0.0500	≥0.0500

Note: Modified from De Paz et al. (2006)

of decision rules and its condition. The constructed decision tree provided an overall accuracy of the model-based inference statistic at 87.60%. Basically, the model-based inference statistic is not concerned with the accuracy of the thematic map but it is concerned with estimating the error of the model that applies to generate the thematic map. The model-based inference statistic can provide the user with a quantitative assessment of each classification decision (Stehman, 2000).

In this study, the classified LULC map in 2015 with an optimum CART model was performed for thematic accuracy assessment using 152 sample points with stratified random sampling from a ground survey in July 2015. As a result, it revealed that the overall accuracy was 87.50% and the Kappa hat coefficient was 80.10%. Meanwhile, the producer's accuracy, which represents omission error, varied between 57.14% for sugarcane and 100.00% for the urban and built- up area, water body, scrub and miscellaneous land. In the meantime, the user's accuracy, which represents commission error, varied between 50.00% for the urban and built-up area and 100.00% for disturbed deciduous forest, water body, and scrub. Based on Fitzpatrick-Lins (1981), a Kappa hat coefficient more than 80% represents strong agreement or accuracy between the predicted map and the reference map.

Distribution of the final LULC classification in 2015 is displayed in Figure 5. It was found that the top 3 dominant LULC classes were cassava, maize, and miscellaneous land and they covered areas of 322.21 km^2, 31.54 km^2, and 25.35 km^2 or 69.30%, 6.78%, and 5.45% of the total study area, respectively. In addition, it was found that the pattern and area of the classified LULC data in this study, particularly agricultural land, was similar to the land use data of the LDD in 2015 (Figure 6).

Soil Erosion Assessment and Its Severity

The main results of the 4 operating functions of the RMMF model included (a) kinetic energy of rainfall (KE), (b) annual runoff (Q), (c) total particle detachment (D)

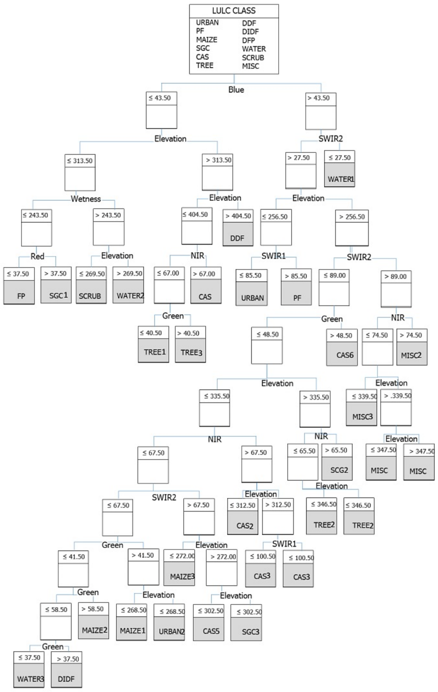

Figure 4. Decision tree structure for LULC classification

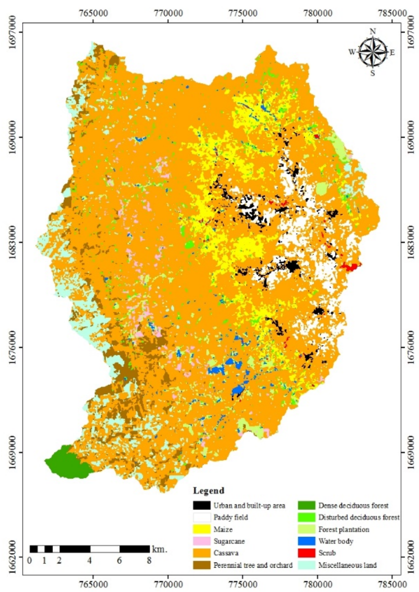

Figure 5. Distribution of LULC classification in 2015

and (d) transport capacity of runoff (TC) and are presented in Figure 7. As a result, it can be observed that the kinetic energy of rainfall varied between 0 and 40517 J m^{-2}, annual runoff varied between 0 and 1030 mm, total particle detachment varied between 0 and 373 kg m^{-2}, and transport capacity of runoff varied between 0 and 2887 kg m^{-2}. Basically, the estimated total particle detachment represents soil loss rates showing the detachment capability by raindrop impact and runoff while the estimated transport capacity of runoff represents soil loss rates reflecting the transport potential in the study area.

The estimation of soil loss by minimum comparison between the estimated total detachment data and transport capacity data is presented in Figure 8(a). It was found that the average soil loss in the study area was 3.368 ton/ha/year with the minimum soil loss of 0 ton/ha/year over the urban and built-up area and water body while the maximum soil loss of 278.196 ton/ha/year was over miscellaneous land (soil pit, sand pit, and land fill). The most dominant soil loss severity class according to the LDD standard was very slightly eroded (≤6.25 ton/ha/year) and it covered an area of 437.70 km^2 or about 94.14% of the total study area (Figure 8(b)). In contrast, the moderately and highly eroded classes covered areas of 17.98 km^2 and 0.31 km^2 or 3.87% and 0.06% of the total study area, respectively (Table 7).

In addition, according to overlay analysis between the soil erosion severity classification and LULC data in 2015, the top 3 dominant crops in the very slightly eroded class were cassava, maize, and paddy field. Conversely, the moderate and highly eroded classes were mostly found in miscellaneous land, which includes soil pit, sand pit, and land fill, and they covered areas of 14.96 km^2 and 0.25 km^2 or 3.22% and 0.05% of the study area, respectively. These results reflect the effect of the LULC on the soil erosion process. Herein, miscellaneous land generates higher soil erosion than other LULC types.

Furthermore, according to the overlay analysis between the soil erosion severity and elevation classifications (Figure 9(a)), it is revealed that most of the very slightly eroded class is situated between 250 m and 350 m and it covered an area of 362.18 km^2 or 77.89% of the total study area. In contrast, the moderately and highly eroded classes were frequently found between 350 and 750 m above mean sea level and they covered areas of 11.62 km^2 and 0.28 km^2 or 2.50% and 0.06% of the total study area, respectively (Table 8). Similarly, according

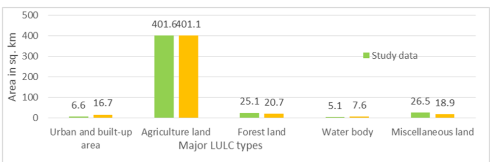

Figure 6. Comparison of area of main LULC types between LDD data in 2015 and this study

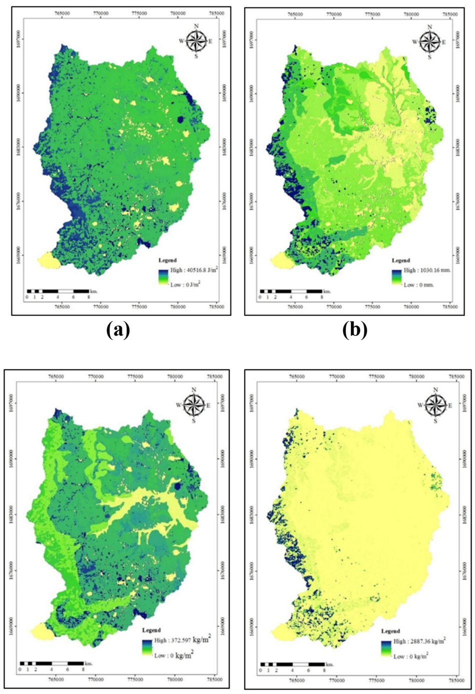

Figure 7. Distribution of kinetic energy of rainfall (a), annual runoff (b), total particle detachment (c), and transport capacity of runoff (d) in the study area

to the overlay analysis between the soil erosion severity and slope classifications for landform (Figure 9(b)), it showed that most of the very slightly eroded class is located at slightly undulating landform (2-5%) and it covered an area of 224.91 km^2 or 48.37% of the total study area. Meanwhile, the moderately and highly eroded classes were frequently found at undulating landform (5-12%) and they covered areas of 9.63 km^2 and 0.16 km^2 or 2.07% and 0.03% of the total study area, respectively (Table 9). In addition, the most dominant soil loss severity class at hilly (20-35%) and steep (>35%) landforms was very slightly eroded because those areas are mostly covered by dense deciduous forest. These findings clearly emphasize the effect of elevation and landform on the soil erosion process in the study area.

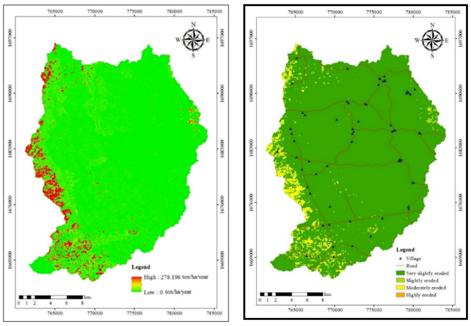

(a) (b)

Figure 8. Distribution of soil erosion (a) and soil erosion severity classification (b)

Herein, soil erosion was very slight since the most dominant elevation class was rather low (250-350 m) and the most dominant landforms were flat or almost flat and slightly undulating.

Optimum Model for EC Estimation

According to the accuracy assessment of the EC data from the candidate linear and non- linear equations with the analyzed EC validation dataset using the NRMSE, the multiple linear equation: Model 1 ($Y = -5.270 - 0.000008*SI_2 + 1.531523*S_1 + 0.047627*S_3 - 0.002451*S_4 + 0.043484*S_5 + 0.013310*S_6$) provided the highest accuracy for the EC estimation with the NRMSE of 0.35235 (Table 10). So, it was chosen as an optimum model for the EC estimation. The optimum equation showed a positive correlation among S_1, S_3, S_5, and S_6 and the EC data and gave a negative correlation among SI2 and S_4 and the EC data. Here, S_1 provided the highest positive influence on the EC data with a coefficient value of 1.531523. The distribution of the estimated EC data in the study area is displayed in Figure 10(a). It revealed that the lowest EC value was - 1.602 dS m^{-1}, the highest EC value was 0.785418 dS m^{-1}, and the average EC value of the study area was 0.785 dS m^{-1}.

Soil Salinity Assessment and Its Severity

The derived EC data, which was estimated using the multiple linear equation: Model 1, was further applied to classify the

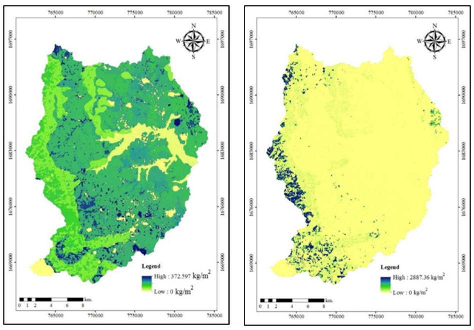

(a) (b)

Figure 9. Distribution of elevation classification (a) and slope classification for landform (b)

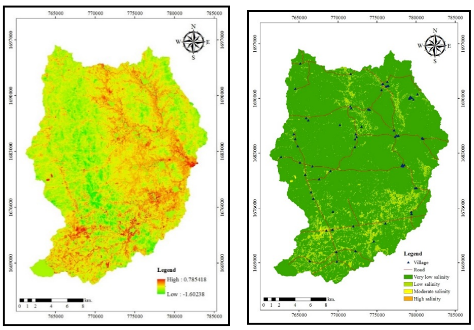

(a) (b)

Figure 10. Distribution of soil electric conductivity estimation (a) and soil salinity severity classification (b)

soil salinity severity with the soil texture (Table 4) and the results are shown in Figure 10(b). The area and percentage of soil salinity severity classification in the study area is summarized in Table 11.

As a result, the most dominant soil salinity severity class was very low and it covered an area of 415.55 km^2 or about 89.374% of the total study area. In contrast, the high soil salinity class only covered an area of 0.01 km^2 or about 0.002% of the total study area. In addition, the total soluble salts (TSS) varied between 0-0.03%. These findings imply that the effect of soil salinity in the Upper Lamchiengkrai watershed is very low and it can be negligible.

In addition, according to the overlay analysis between the soil salinity severity classification and the LULC data in 2015, the top 3 dominant crops in the very low soil salinity class were cassava, maize, and paddy field. In contrast, the moderate and high salinity classes were mostly found in cassava areas and they covered areas of 2.06 and 0.01 km^2 or 0.443 and 0.002% of the study area, respectively.

Table 7. Area and percentage of soil loss severity classification in the study area

No.	Soil loss severity class	Erosion rate (t/ha/y)	Area in km^2	Percent
1	Very slightly eroded	≤6.25	437.70	94.14
2	Slightly eroded	6.26-31.25	8.97	1.93
3	Moderately eroded	31.26-125.00	17.98	3.87
4	Highly eroded	125.01-625.00	0.31	0.06
	Total		**464.96**	**100.00**

Table 8. Relationship between soil loss severity and elevation

Elevation classes	Soil loss severity classes							
	Very slightly eroded		Slightly eroded		Moderately eroded		Highly eroded	
	Km^2	%	Km^2	%	Km^2	%	Km^2	%
< 200 m	0.48	0.10	0.05	0.01	0.06	0.01	0.00	0.00
200-250 m	51.87	11.16	0.00	0.00	0.02	0.00	0.00	0.00
250-350 m	362.18	77.89	4.70	1.01	6.28	1.35	0.04	0.01
350-750 m	23.18	4.99	4.22	0.91	11.62	2.50	0.28	0.06
Total	437.70	94.14	8.97	1.93	17.98	3.87	0.31	0.07

Table 9. Relationship between soil loss severity and landform

Landform by slope classes	Soil loss severity classes							
	Very slightly eroded		Slightly eroded		Moderately eroded		Highly eroded	
	Km^2	%	Km^2.	%	Km^2	%	Km^2	%
Flat or almost flat (0-2%)	137.74	29.63	1.93	0.42	0.54	0.12	0	0
Slightly undulating (2-5%)	224.91	48.37	3.69	0.79	7.51	1.62	0	0
Undulating (5-12%)	71.46	15.37	2.97	0.64	9.63	2.07	0.16	0.03
Rolling (12-20%)	1.47	0.32	0.19	0.04	0.13	0.03	0.11	0.02
Hilly (20-35%)	1.35	0.29	0.07	0.02	0.01	0	0.03	0.01
Steep (>35%)	0.77	0.17	0.12	0.03	0.16	0.04	0.01	0
Total	**437.70**	**94.14**	**8.97**	**1.93**	**17.98**	**3.87**	**0.31**	**0.07**

Optimum Model for Soil Organic Matter Estimation

According to the accuracy assessment of the soil organic matter data from the candidate linear and non-linear equations with the analyzed OM validation dataset using the NRMSE, the multiple linear equation: Model 3 (Y = 1.058 - 0.607 * Band2 + 0.777 * Band3 - 0.147 * Band4 - 0.032 * Band5 + 0.008 * Band6 - 0.011 * Slope + 73.963 * CI - 61.988 * SI) provided the highest accuracy for the soil organic matter estimation with the NRMSE of 0.29744 (Table 12). So, it was chosen as an optimum model for the OM estimation. The optimum equation showed a positive correlation among Band 3, Band 6, and the coloration index (CI) and OM data and gave a negative correlation among Band 2, Band 4, Band 5, Slope, and the salinity index (SI) and OM data. Here, the CI provided the highest positive influence on the soil organic matter with a coefficient value of 73.963. This finding is consistent with the previous work of Mandal (2015) who applied spectral color indices to predict soil organic matter content from remotely sensed data in Nepal. He mentioned that the CI was a significant predictor variable for the OM prediction.

The distribution of the estimated OM in the study area is displayed in Figure 11(a). It was found that the lowest OM value was -0.91848% and the highest OM value was 2.33499% while the average OM value of the study area was 0.94295%. In the meantime, the

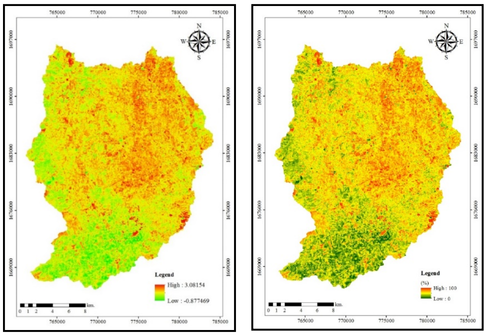

(a) (b)

Figure 11. Distribution of soil organic matter estimation (a) and soil organic matter in percent (b)

Table 10. List of candidate equations of linear and non-linear regression analysis and accuracy assessment for optimum EC estimation model identification

Linear and non-linear regression	Equation	R^2	RMSE	NRMSE	Rank
Simple linear model	Y =- * 043.0 + 894.1S5	0.502	0.13927	0.36193	3
Multiple linear: Model 1	Y = -*000008.0 - 270.5SI*531523.1 + 2S + 1 *047627.0S*002451.0 - 3S*043484.0 + 4S + 5 *013310.0S6	0.521	0.13559	0.35235	1
Multiple linear: Model 2	Y = -*000008.0 - 412.5SI*618453.1 + 2S + 1 *047424.0S*042294.0 + 3S*013517.0 + 5S6	0.521	0.13802	0.35868	2
Quadratic model	Y = 22.576 + (-1.015 * S5) + (0.011 * S5 **2)	0.611	0.86581	2.25003	4
Cubic model	Y = 6.960 + (-0.011 * S5 **2) + (0.000 * S5 **3)	0.612	16.35473	42.50190	5

Table 11. Area and percentage of soil salinity severity classification in the study area

No.	Soil salinity severity class	Effect on Plant Growth	Total soluble salts in %	Km^2	Percent
1	Very low	Negligible effect	0-0.03	415.55	89.374
2	Low	Very sensitive crops affected	0.01-0.03	47.34	10.181
3	Moderate	Many crops affected	0.02-0.04	2.06	0.443
4	High	Salt tolerant plants grow	0.04-0.05	0.01	0.002
		Total		**464.96**	**100.000**

estimated OM data that was normalized and converted in percent for the BDI calculation is presented in Figure 11(b).

Soil Biological Degradation Assessment and Its Severity

The BDI that was derived from the soil organic matter in percent using Equation 15 is presented in Figure 12(a) and the soil biological degradation classes according to the values (Table 6) are shown in Figure 12(b). Meanwhile the area and percentage of soil biological degradation classification is summarized in Table 13.

The result showed that the most dominant soil biological degradation class was moderate degradation and it covered an area of 296.05 km^2 or 63.67% of the total study area. According to the overlay analysis between the soil biological degradation classification and the LULC data in 2015, the most dominant crop that was situated in the moderate soil degradation class was cassava and it covered an area of 214 km^2 or 46.025% of the total study area. This phenomenon was also present in the high and very high soil biological degradation classes. These findings reflect an intensive use of soil for agricultural activities in the Upper Lamchiengkrai watershed, particularly cassava cultivation.

Soil Degradation Assessment and Its Severity

According to the combination of the normalized 3 indicators on soil degradation (soil loss, soil salinity, and soil biological degradation) using the multiplicative method, the most dominant soil degradation class in the study area was very low and it covered an area of 443.00 km^2 or 95.278% of the total study area, whereas the high and very high soil

Table 12. List of candidate equations of linear and non-linear regression analysis and accuracy assessment for optimum OM estimation model identification

Linear and non-linear regression	Equation	R^2	RMSE	NRMSE	Rank
Simple linear	Y = 3.262 - 0.038 * Band5	0.553	0.65023	0.29964	6
Multiple linear: Model. 1	Y = -5.298 - 0.618 * Band2 + 0.890 * Band3 - 0.149 * Band4 -0.034 * Band5 + 0.014 * Band6 - 0.007 * Band7 - 0.010 * Slope + 71.046 * CI + 3941.633 * RI - 66.852 * SI	0.618	0.64630	0.29783	2
Multiple linear: Model. 2	Y = 0.933 - 0.655 * Band2 + 0.810 * Band3 - 0.127 * Band4 - 0.034 * Band5 + 0.013 * Band6 - 0.008 * Band7+ - 0.010 * Slope + 76.431 * CI - 65.738* SI	0.617	0.64438	0.34904	10
Multiple linear: Model. 3	Y = 1.058 - 0.607 * Band2 + 0.777 * Band3 - 0.147 * Band4 - 0.032 * Band5 + 0.008 * Band6 - 0.011 * Slope + 73.963 * CI - 61.988 * SI	0.615	0.64544	0.29744	1
Multiple linear: Model. 4	Y = 0.905 - 0.613 * Band2 + 0.814 * Band3 - 0.174 * Band4 -0.033 * Band5 + 0.007 * Band6 + 77.066 * CI - 62.835 * SI	0.611	0.64752	0.29840	5
Multiple linear: Model. 5	Y = 0.367 - 0.609* Band2 + 0.859 * Band3 - 0.201 * Band4 - 0.029 * Band5 + 81.990 * CI - 63.638 * SI	0.604	0.64673	0.29803	3
Multiple linear: Model. 6	Y = 1.279 + 0.123 * Band3 - 0.091 * Band4 - 0.032 * Band5 + 17.632 * CI - 8.779 * SI	0.595	0.64695	0.29813	4
Multiple linear: Model. 7	Y = 1.173+0.036 * Band3+ -0.033 * Band5+ 10.614 * CI + -9.463* SI	0.591	0.65049	0.29976	7
Multiple No. 8	Y = 2.026 - 0.041 * Band5 + 0.032 * Band2	0.571	0.66060	0.30442	9
Cubic model	Y = 4.251 - 0.062 * Band5 + 0.000002 * Band5**3	0.557	0.65929	0.30382	8
Quadratic model	Y = 4.597 - 0.081 * Band5 + 0.000 * Band5**2	0.556	1.47980	0.68194	13
Growth model	Y = e** 3.313 - 0.057 * Band5	0.516	0.75756	0.34910	12
Exponential model	Y = 27.457 * e** - 0.057 * Band5	0.516	0.75741	0.34904	11

degradation classes only covered areas of 0.45 km^2 and 0.01 km^2 or 0.096% and 0.003%, respectively, of the total study area (Figure 13 and Table 14). As a result, it can be observed that the pattern of soil degradation classification was similar to the normalized soil erosion.

In addition, according to the overlay analysis between the soil degradation classes and the LULC data in 2015, the top 3 dominant crops in the very low soil degradation severity class were cassava, maize, and paddy field. Conversely, the high and very high soil degradation severity classes were mostly found in miscellaneous land (soil pit, sand pit, and land fill). This finding was true because the soil of miscellaneous land, in general, is very poor.

Finally, it can be concluded that a soil degradation problem does not exist in the study area since the severity of soil erosion and salinity were very low while the soil biological degradation was moderate.

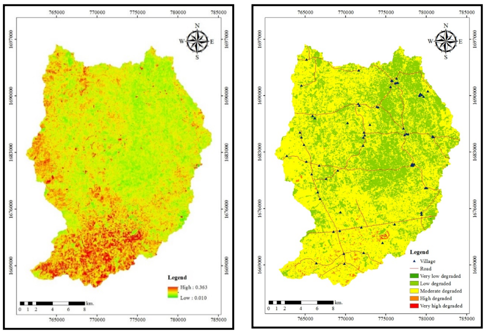

(a) (b)

Figure 12. Distribution of soil biological degradation index (a) and soil biological degradation classification (b)

Conclusions

The soil degradation assessment in 2015 was here successfully implemented by the integration of 3 indicators: soil erosion, soil salinity, and soil biological degradation using geoinformatics technology, particularly remote sensing, GIS, and GPS. The spatial distribution of the 3 indicators on soil degradation and their severity classifications were displayed and quantified in terms of area and percentage. These findings can be used as a guideline for soil scientists to assess soil degradation in the future.

Table 13. Biological degradation index and soil biological degradation classification

No	Level of soil biological degradation	BDI (Unit less)	Area in km^2	Percent
1	Very low	0-0.3	0.28	0.06
2	Low	0.3-0.6	163.43	35.15
3	Moderate	1	296.05	63.67
4	High	1-2.5	5.12	1.10
5	Very High	>2.5	0.08	0.02
	Total		**464.96**	**100.00**

Table 14. Area and percentage of soil degradation severity classification

No.	Severity class of soil degradation	Area in km^2	Percent
1	Very low	443.00	95.278
2	Low	11.67	2.510
3	Moderate	9.83	2.114
4	High	0.45	0.096
5	Very High	0.01	0.003
	Total	**464.96**	**100.000**

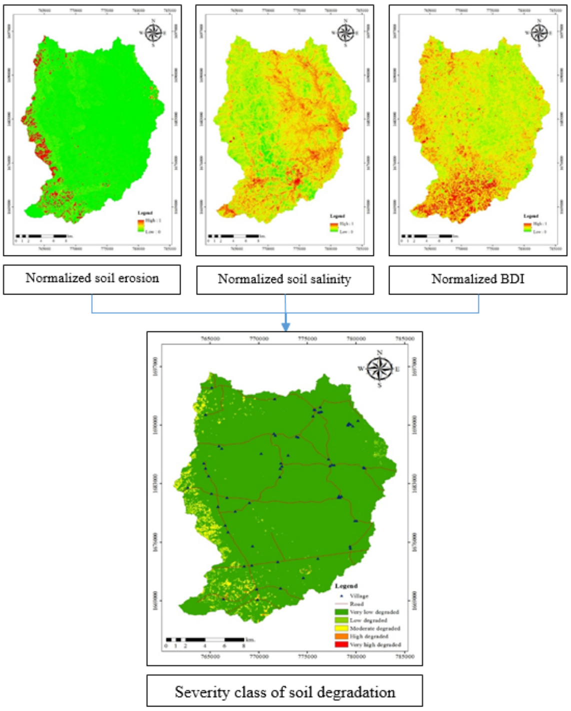

Figure 13. Distribution of soil degradation severity classification

In a nutshell, it can be concluded that geoinformatics technology can be efficiently used as a tool to assess soil erosion, soil salinity, soil organic matter depletion, and their severities for soil degradation assessment. The developed research methodology was more effective than the traditional approach because it can save labor, cost, time, and effort and data can be quickly assessed.

References

Abbas, A. and Khan, S. (2007). Using remote sensing techniques for appraisal of irrigated soil salinity. In: Advances and Applications for Management and Decision Making in Land, Water and Environmental Management. Oxley, L. and Kulasiri, D., (eds). Modelling and Simulation Society of Australia and New Zealand, Christchurch, New Zealand, p. 2632-2638.

Bai, Z.G., Dent, D.L., Olsson, L., and Schaepman, M.E. (2008). Proxy global assessment of land degradation. Soil Use Manage., 24:223-234.

De Paz, J.M, Sánchez, J., and Visconti, F. (2006). Combined use of GIS and environmental indicators for assessment of chemical, physical and biological soil degradation in a Spanish Mediterranean region. J. Environ. Manage., 79:150-162.

Douaoui, A.E.K., Nicolas, H., and Walter, C. (2006). Detecting salinity hazards within a semiarid context by means of combining soil and remote sensing data. Geoderma, 134:217-230.

Eaton, D. (1996). Unpublished data. Environmental Economics Programme. International Institute for Environmental and Development, London, UK.

Fadhil, M.A. (2009). Land degradation detection using geo-information technology for some sites in Iraq. J. Al-Nahrain Uni., 12(3):94-108.

Food and Agriculture Organization of the United Nations. (2005). The Importance of Soil Organic Matter Key to Drought-Resistant Soil and Sustained Food Production. FAO, Publishing Management Service, Rome, Italy, 95p.

Fitzpatrick-Lins, K. (1981). Comparison of sampling procedures and data analysis for a land-use and land cover map. Photogramm. Eng. Rem. S., 47(3):343-351.

Gao, B-C. (1996). NDWI-A normalized difference water index for remote sensing of vegetation liquid water from space. Remote Sens. Environ., 58:257-266.

Harmsen, K. (1996). Assessment of current erosion damage. Lang Druck AG, Liebefeld, Bern, Switzerland, 111p. Quoted in Yazidhi, B. (2003). A comparative study of soil erosion modeling in Lom Kao-

Phetchabun, Thailand, [MSc. thesis]. Faculty of Geoinformation Science and Earth Observation, University of Twente, Enschede, Netherlands, 104p.

Huete, A. (2004). Remote sensing of terrestrial ecosystems. In: Remote Sensing for Natural Resource Management and Environmental Monitoring. 3rd ed. Ustin, S.L., (ed). John Wiley & Sons, Hoboken, NJ, USA, p. 1-52.

Jumpa, K. (2012). Unpublished data. Land Development Department, Ministry of Agriculture and Cooperatives, Bangkok, Thailand.

Kamonrat, T. and Jirakajohnkool, S. (2012). The application of geo-information technology and mathematic model for soil erosion assessment in the Upper Lam Phra Phloeng Watershed, Nakhon Ratchasima Province, Thailand. Thammasat Int. J. Sci. Tech., 20(2):167-177. (in Thai)

Kapalanga, T.S. (2008). A review of land degradation assessment methods. Land Restoration Training Programme, p. 17-68.

Kapalanga, T.S. (2009). A review of land degradation assessment & monitoring methods. Proceedings of the 13th Namibian Rangeland Forum Conference: The role of biodiversity in rangeland management and policy biodiversity in rangeland management and policy; October 27-28, 2009; Windhoek, Namibia.

Katawatin, R. and Sukchan, S. (2012). Mapping of soil salinity and soil erosion in Thailand with emphasis on computer-assisted techniques. Pedologist, p. 343-354.

Khan, N.M., Rastoskuev, V.V., Sato, Y., and Shiozawa, S. (2005). Assessment of hydrosaline land degradation by using a simple approach of remote sensing indicators. Agr. Water Manage., 77:96-109.

Lal, R. (1998). Soil quality and sustainability. In: Methods for Assessment of Soil Degradation. Lal R., Blum, W.H., Valentine, C., and Stewart B.A., (eds). CRC Press, Boca Raton, FL, USA.

Land Development Department. (2002). Land degradation project approach. Available from: www.ldd.go.th/Efiles_project/ldd_planning/welcome/index.html. Accessed date: March 8, 2013.

Land Development Department. (2000). Soil Loss Map of Thailand. Land Development Department, Ministry of Agriculture and Cooperatives, Bangkok, Thailand, 47p.

Land Development Department. (2015). State of Soil and Land Resources of Thailand. Land Development Department, Ministry of Agriculture and Cooperatives, Bangkok, Thailand, 88p.

Lillesand, T.M., Kiefer, R.W., and Chipman, J.W. (2004). Remote Sensing and Image Interpretation. Wiley, NY, USA, 763p.

Mainguet, M. (1994). Desertification: Natural Background and Human Mismanagement. Springer-Verlag, Berlin, Germany, 314p. Quoted in Denti, G.D. (2004). Developing a desertification indicator system for a small Mediterranean catchment: A case study from the Serra De Rodes, Alt Emporda, Catalunya, NE Spain, [Ph.D. thesis]. Department of Chemical Engineering, Agriculture and Food Technology, University of Girona, Girona, Spain, 406p.

Mandal, U.K. (2015). Spatial prediction of soil organic matter content using remote based spectral color indices, Nepal. Proceedings of the International Federation of Surveyors (FIG) 2005, p. 1-10. Available from: https://www.fig.net/resources/proceedings/2015/2015_11_nepal/T.S.4.5.pdf

Mathieu, R. and Pouget, M. (1998). Relationships between satellite-based radiometric indices simulated using laboratory reflectance data and typic soil color of an arid environment. Remote Sens. Environ., 66:17-28.

Mhangara, P. (2011). Land use/cover change modeling and land degradation assessment in the Keiskamma catchment using remote sensing and GIS, [Ph.D. thesis]. Faculty of Science, Nelson Mandela Metropolitan University, Port Elizabeth, South Africa, 187p.

Morgan, R.P.C. (2001). A simple approach to soil loss prediction: a revised Morgan–Morgan–Finney model. Catena, 44:305-322.

Morgan, R.P.C. and Duzant, J.H. (2008). Modified MMF (Morgan-Morgan-Finney) model for evaluating effects of crops and vegetation cover on soil erosion. Earth Surf. Proc. Land., 32:90-106.

Patterson, R.A. (2006). Consideration of soil salinity when assessing land application of effluent. Septic Safe Technical Sheet 01/2 NSW Department of Local Government. Available from: www.dlg.nsw.gov.au. Accessed date: Jan 15, 2013.

Prince, S.D. (2002). Spatial and temporal scales for identification of desertification. In: Global Desertification: Do Humans Cause Deserts? Reynolds, J.F. and Stafford Smith, D.M., (eds). Dahlem Workshop Report 88, Dahlem University Press, Berlin, Germany, 24-37. Quoted in Mambo, J. and Archer, E. (2006). An assessment of land degradation in the Save catchment of Zimbabwe. Area, 39(3):380-391.

Rouse, J., Haas, R., Schell, J., Deering, D., and Harlan, J. (1974). Monitoring the Vernal Advancement and Retrogradation (Greenwave Effect) of Natural Vegetation. Texas A & M University, College Station, TX, USA, 362p.

Sethabut, P. (2008). Green mirror desertification. Available from: http://library.cmu.ac.th/ntic/knowledge_show.php?docid=20. Accessed date: August 10, 2014.

Singh, B.K., Verma, K., and Thoke, A.S. (2015). Investigations on impact of feature normalization techniques on classifier's performance in breast tumor classification. Int. J. Comput. Appl. T., 116(19):11-15.

Stehman, V.S. (2000). Practical implications of designed-based sampling inference for thematic map accuracy assessment. Remote Sens. Environ., 72:35-45.

Suriyaprasit, M. (2008). Digital terrain analysis and image processing for assessing erosion prone areas: A case study of Nam Chun Watershed, Phetchabun, Thailand, [MSc. thesis]. Faculty of Geo-Information Science and Earth Observation, International Institute for Geo-information Science and Earth Observation, Enschede, Netherlands, 85p.

Torahi, A.A. (2012). Rangeland dynamics monitoring using remotely sensed data, in Dehdez Area, Iran. Proceedings of the International Conference on

Applied Life Sciences; September 10-12, 2012; Konya, Turkey, p. 10-12.

Torrion, J.A. (2002). Land degradation detection, mapping and monitoring in the Lake Naivasha Basin, Kenya, [MSc. thesis]. Faculty of Geo-Information Science and Earth Observation, International Institute for Geoinformation Science and Earth Observation, Enschede, Netherlands, 94p.

United Nations Environment Programme. (2006). Africa Environment Outlook 2: Our Environment, Our Wealth. UNEP/Earthprint, United Nations Environment Programme, Nairobi, Kenya, 542p.

Yazidhi, B. (2003). A comparative study of soil erosion modeling in Lom Kao-Phetchabun, Thailand, [MSc. thesis]. Faculty of Geo-information Science and Earth Observation, International Institute for Geo-information Science and Earth Observation, Enschede, Netherlands, 104p.